Conceptual Design of a Near-Future Laser ICF Driver “Pulsar”

By Ye Junchi (China)
finnleykepler@gmail.com

Abstract

The use of Fusion as the energy source of a rocket propulsion system has great potential to significantly reduce travel times to the outer planets [3]. Research into this has been focused on more far-future and exotic fusion drives [9], while recent research efforts into near future fusion drives focus mainly on Zeta-Pinch or direct fusion [10−12]. However, Inertial-confinement fusion (ICF) could also be a viable option [3]. This paper is a proposal of a conceptual fusion drive - “Pulsar”. Studies include the selection of fuel options (D-T and D-3He), concept, thermal-mechanical properties, theoretical performance, and applications compared to other options. A combination of Deuterium-Tritium (D-T) fuel, reflected fiber pulse laser system, spin-aligned frozen fusion pellets, and a Tantalum-Hafnium Carbide (TaHfC) heat shield shows great promise for a viable near-future ICF propulsion system.

“Keywords” D-T, Conceptual design, Near-future, Laser confinement, Inertial Confinement Fusion, Fusion Driver

1. Introduction

The study of fusion energy for the means of propulsion started ever since the first years of fusion research. Most proposed concepts show great promise for a manned mission to the stars (given we solve cryosleep), requiring great technological advancements and an unreasonable amount of funding to make it feasible [9]. However, only a handful of concepts are designed for the use of interplanetary travel [3, 10, 12], specifically for a manned mission to the outer planets (Jupiter, Saturn, Uranus, Neptune, and Pluto). Most of such concepts are designed to use Zeta-Pinch fusion or direct fusion with the use of microwave heating. Zeta-Pinch fusion has undesirable neutron flux and plasma instabilities that limits its power output [11], and dedicating a significant mass fraction of the spacecraft for thermal management. Direct fusion drives have an unreasonably low thrust-to-weight ratio [12], making a mission to the outer planets difficult as it will be difficult to accelerate and especially slow down. Additionally, a DFD has an extremely low specific impulse when compared to other fusion drives.

An ICF Drive benefits from: wide range of power variations (pulse rate changes), high thrust power : waste heat ratio, and a reduction of radiation exposure to reactor components. When compared to other fusion drivers (Zeta-Pinch, Direct Fusion, Linear Fusion, Mirror Cell, Toroidal Tokamak) Inertial Confinement has the least amount of energy transfer to reactor components, resulting in high exhaust velocities, and low waste heat output, significantly increasing overall spacecraft ΔV.

Similar concepts such as the “Vehicle for Interplanetary Space Transport Application” (VISTA) have explored possibilities with a basic inertial confinement system consisting of a conically shaped thruster, lasers mirrored to the detonation point, with a magnetically redirected exhaust of charged particles [3]. This is insufficient, as the fuel choice for the VISTA fusion drive, D-T, releases most of its energy in its neutron products [1, 3], which cannot be redirected into thrust via a magnetic nozzle due to its neutral electromagnetic charge. The neutrons radiate in all directions, causing heat transfer to the driver components, and neutron embrittlement [2]. This mitigates the advantages of ICF drivers. “Pulsar” utilizes the same D-T fuel combination, but using magnetic spin alignment for neutron redirection to mitigate heat flux, neutron activation, and neutron embrittlement; A hollow hemispherical Tantalum-Hafnium Carbide (TaHfC) heat shield with a high emissivity constant (14.5MW/m² @4000K) [1], allowing thermal equilibrium of absorbed reaction heat and radiated heat, further reducing spacecraft size and mass.

This design involved in this paper is purely conceptual, with a list of assumptions made to simplify the driver system. Comprehensive studies into specific components of the fusion driver is outside the scope of this paper. This paper will only outline the loose requirements of the fusion driver components. Certain components are given assumed construction and materials from similar component counterparts used in other fields, Ex. MRI machines.

2. Table of Assumptions for the Fusion Driver "Pulsar"

Reaction Properties (R)

R-1: For D-T reactions, P. Gamma, Bremsstrahlung, and Synchrotron are treated as negligible. [5]

R-2: Side reaction fractions (D-D, D-D+T, etc.) are considered negligible.

R-3: Complete detonation and utilization of all fuel in the pellet.

Material (M)

M-1: An ideal insulator is used to insulate the heat shield from the ship. [7]

M-2: Sufficient structural support for TaHfC tiles can be installed with negligible heat transfer. (M1)

Laser Properties (L)

L-1: Inertial confinement detonation laser efficiency of ~50%

L-2: Laser system has a output power density of $\sim 10^{16}$W/cm, identical to that of the NIF [4],

L-3: Laser driver mass to pulse power ratio of 0.7 kw/kg

Spin Alignment Properties (S)

S-1: Almost total spin alignment is possible at temperatures near 0K

S-2: Spin alignment is maintained if fuel pellets were flash-heated

S-3: Spin alignment will reduce heat shield neutron flux by >55%

S-4: Neutron exhaust beam cosine losses assumed to be ~0.293 (1 - cos 45°)

S-5: Losses in spin alignment from bumping and pellet injector is included in S-1.

3. The Ideal Energy Source and The Obtainable Energy Source

Energy sources for an ICF driver can vary, but the most promising two reactions with low enough activation energy are Deuterium - Tritium (D-T), and Deuterium - Helium-3 (D-^{3}He).

$$D\text{-}T + 50keV \rightarrow 17.6\ MeV + {}^4He(3.5\ MeV) + n(14.1\ MeV) \quad [1]$$

$$D\text{-}{}^3He + 100keV \rightarrow 18.2\ MeV + {}^4He(3.6\ MeV) + p(14.7\ MeV) \quad [1]$$

The Deuterium - Tritium fuel combination is the easiest to ignite, producing a great deal of energy that produces a theoretical exhaust velocity of ~8.7%c [1]. However, it comes with a major downside: >80.1% of the energy output is kinetic neutron energy [1, 10, 11]. Neutrons are neutrally charged, and therefore cannot be redirected by a magnetic field into thrust. Moreover, neutrons of >14MeV cause neutron embrittlement, with neutron activation that progressively deteriorates the exposed driver components [2, 11], Deuterium is relatively easy to produce through the electrolysis of water and the ammonia-hydrogen isotope exchange process [13]. On other celestial bodies, D2O is widely available in the form of heavy water Ice, therefore the possibility of In-Situ Resource Utilization (ISRU). Tritium can also be produced through lithium neutron activation:

$$Li^6 + n \rightarrow T + {}^4He \quad (Li^6,\ Primary\ n\text{-}activation) \quad [1]$$

$$Li^7 + n \rightarrow T + {}^4He + n \quad (Li^7,\ produced\ by\ n\text{-}activated\ Boron\text{-}10) \quad [1]$$

The resultant Tritium is to be used for fusion reactions, while the Helium can be injected into the exhaust gas flow to produce additional thrust while reducing specific impulse.

Deuterium - Helium-3 is the much more ideal fuel. Being significantly harder to ignite, but producing a theoretical exhaust velocity of ~8.9%c and no neutrons whatsoever (ignoring D-D side reactions) [1]. The products are a Helium-4 nucleus and a proton, both of which are positively charged and can be redirected to produce thrust [1] . However, D-^{3}He releases a great deal of Bremsstrahlung X-rays, with a power ratio PFusion/PBremsstrahlung of ~5.3 (compared to D-T's ~140) [1]. X-rays are difficult to shield, as photons are rays, you can't fully get rid of all of it, but only reduce it to an acceptable level [14]. An attenuation factor for shielding material is proportional to the density of the shielding material, therefore reducing radiation to an acceptable level by increasing the thickness of the shielding material would significantly increase the mass of the spacecraft [14]. Despite this, D-^{3}He drivers are still generally significantly more efficient than D-T. The problem is in fuel availability. Deuterium is no problem, but Helium-3 is an elusive fuel. There are 3 main ways to get Helium-3. Through a D-D reactor (on the ground) that produces Helium-3:

D-D + 500keV → 4.03 MeV + T(1.01 MeV) + p(3.02 MeV) [1]

D-D + 500keV → 3.27 MeV + ^{3}**He(0.82 MeV)** + n(2.45 MeV) [1]

Mining the lunar surface, but as Helium is a noble gas, it refuses to bind to anything to form minerals, therefore the Helium-3 we can find would be in extremely small quantities in gas pockets, insignificant to the amounts necessary for long term spacecraft usage. The final option is to scoop it from the atmosphere of Jupiter or Saturn, which is currently impractical. As it is almost impossible to easily obtain a considerable amount of Helium-3, for the near-future setting of the concept, D-T is selected as the fuel combination.

4. "Pulsar" Fusion Driver Layout

The proposed fusion driver will have 5 major systems: cryogenic, diamagnetic, thermal, laser, and radiation. Liquid Deuterium and Tritium are fed into a fusion pellet freezer. Under a ~10 Tesla magnetic field, the pellets are frozen in the spin-aligned state. The pellets are fed into a pellet injector that will accelerate the pellets to the detonation point to be detonated by 24 reflected laser beams about the equator of the fuel pellet. The resultant neutron flux is reduced by spin alignment and ~53% of neutron "thrust power" is used to produce thrust under "ideal velocities" of 17.1%c when taking cosine losses into account, and ~75.3% of total neutron energy is producing thrust. The charged particles (alpha) will have an exhaust velocity of 4.3%c in the opposite direction, which will require redirection from a magnetic field.

The cryogenic system consists of a cryogenic fuel refrigeration system to keep the tanks <20K, and to chill liquid Helium for superconductor cryostat. Fuel is stored as a liquid, and later frozen into solid pellets when needed. The solid fuel pellet freezing process uses a fusion pellet factory that encapsulates the fuel in a thin plastic film. This plastic film will be later vaporized by the lasers, and the resultant force from Newton's 3rd law of motion will compress the pellet, igniting the fusion reaction. The assembled pellet (plastic film ball with liquid D-T mixture inside) will then be exposed to a 10 Tesla magnetic field as it's cooled to sub-microkelvin temperatures, where the fuel pellet is polarized. Immediately the pellet will be ejected out into the detonation point, where lasers will trigger its detonation. Additionally, the cryogenic system is also used to cool liquid Helium for cooling the diamagnetic system.

The diamagnetic system consists of a series of superconducting magnets. A 10 Tesla Niobium-Titanium superconducting coil for cooling the fuel pellet and spin polarization, and a 3 tesla Niobium-Titanium superconducting coil for shielding the heat shield from charged particles, and redirection of said charged particles to produce thrust.

The thermal system consists of a heat shield, cooling loops, and insulators. The heat shield is a hollow hemisphere 20 m in diameter and ~2-10 mm in thickness that can be assembled in orbit. Specific thicknesses require further studies. A carbon composite sandwiched between two carbon plates can be used as an insulator similar to one found on the Parker Solar Probe [8]. Cooling loops will be connected to the cryogenic cooler, and the hot loop to a power converter to recycle some power before the rest of the energy is radiated.

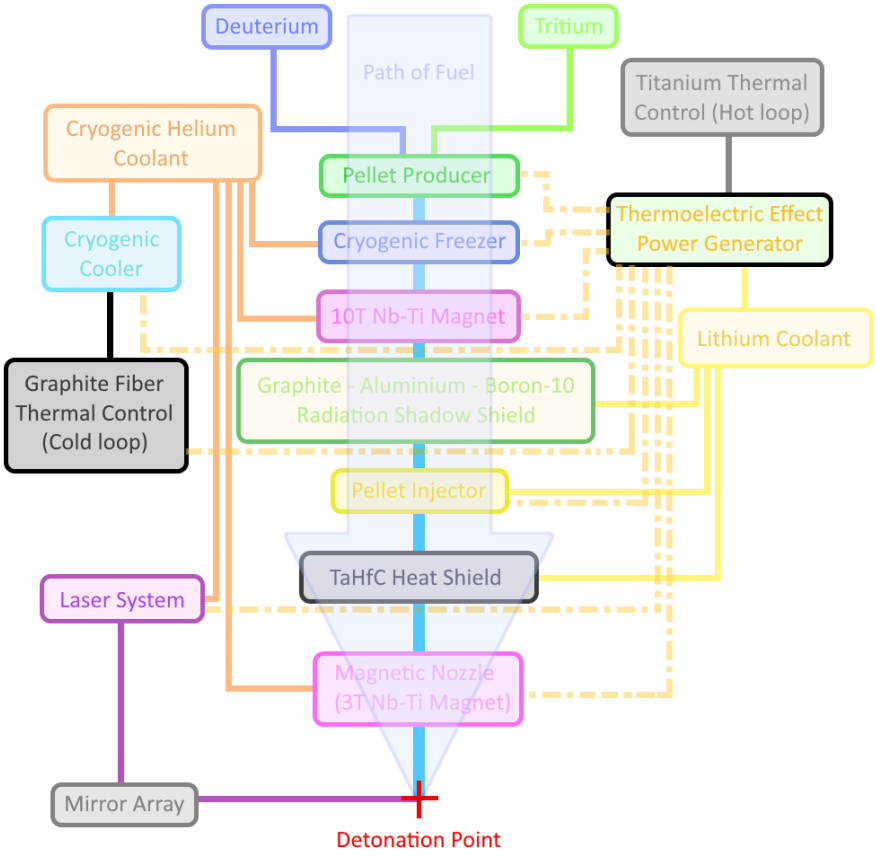

[Fig. An Overview of Engine Layout and Resources]

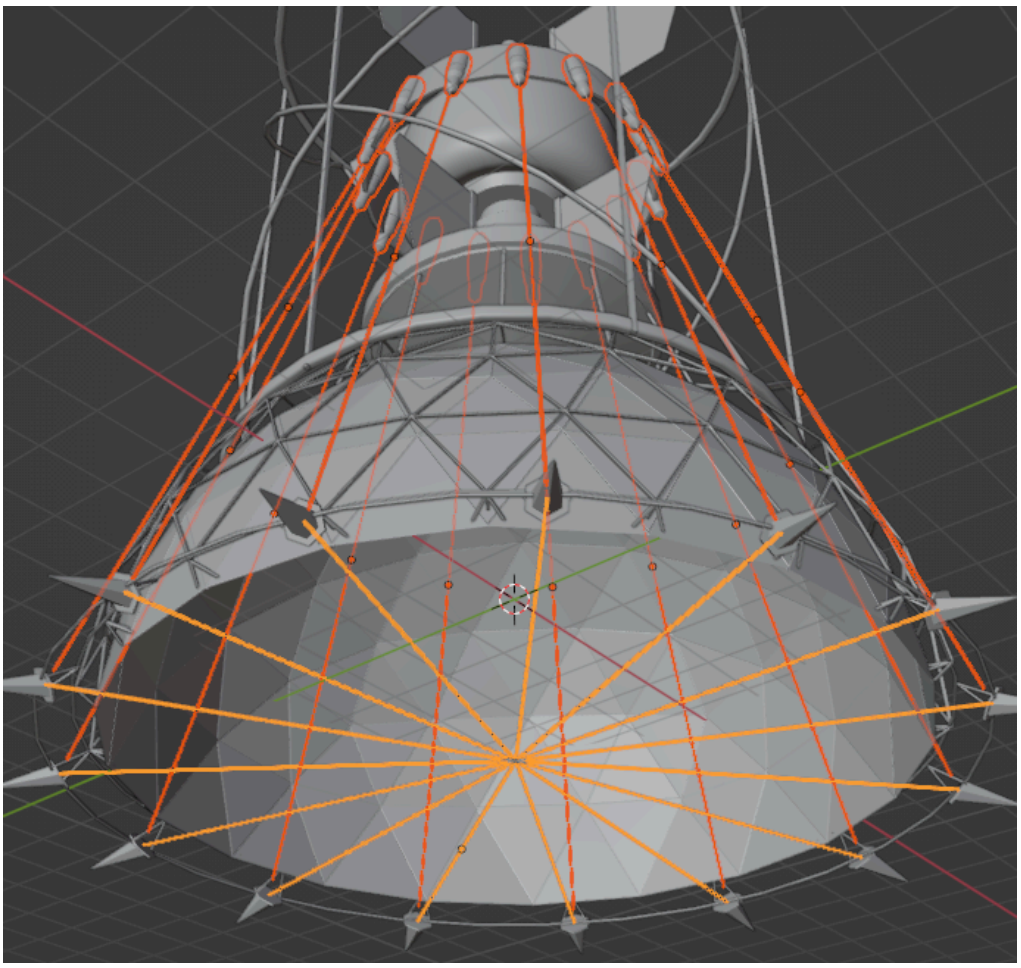

[Fig. B Laser Assembly and Layout]

Nd:glass flash lamp pumped lasers could be used for the laser system due to its technological readiness. Nd:glass lasers that are used in the NIF have a laser efficiency of ~0.5% [4]. This is unacceptable, as the power requirement would be in the gigawatts. In order to power a spacecraft with such an engine with a reasonably sized nuclear reactor, magnetic brake, or thermoelectric effect generator (recycling heat from the heat shield), laser efficiency must be ~50%. This may seem impossible, but the low pulse power requirement could make it feasible with modern fiber lasers with power conversion rates of 30-50% [21]. Lasers are installed in a radial assembly away from the detonation point and behind the shadow shield, its beams are reflected to the detonation point with mirrors. The mirrors need to endure neutron bombardment, therefore a carbon-based reflective surface is preferred. Solid-state spike radiators are placed along the back side of the mirrors to prevent overheating.

Radiation shielding will consist of a graphite reflector layer in front of an aluminium case filled with ^{10}B-Al Alloy powder, placed (insulated) behind the heat shield, creating a shadow of neutron radiation free zone acceptable for onboard electronics and humans. Additionally this radiation shield will also absorb some radiated energy from the heat shield, which will need to be radiated. Some of this heat can be used to generate power through a thermoelectric effect generator.

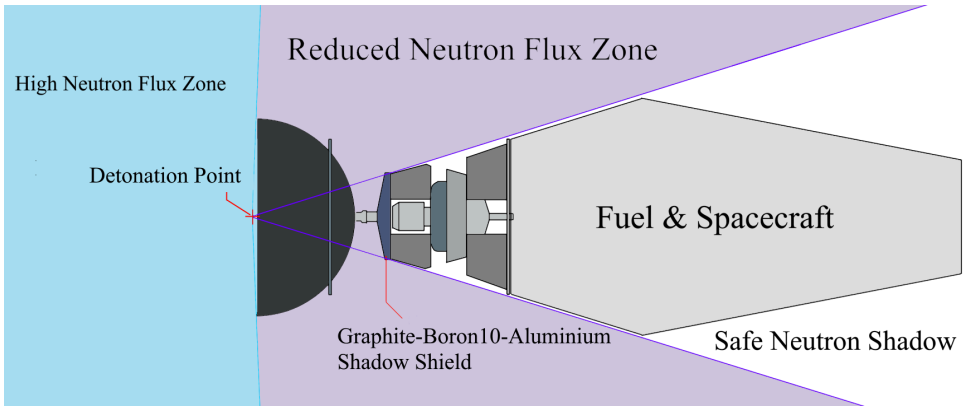

[Fig. C Neutron Flux Zones]

Increasing cooling of the TaHfC heat shield and recycling heat through a thermoelectric effect generator could allow an increase in maximum fusion power output. This is not explored due to the low efficiency of TEGs (solid-state thermal power converters). Using a TEG to recycle power will increase engine dry mass significantly. Increase in cooling of the heat shield would also increase the Titanium hot loop radiator mass, which will also lead to an increase in spacecraft dry mass. The exact parameters are not explored as it may vary depending on spacecraft design. Do consider this as a modifiable parameter of the driver.

Another theoretical option is the installation of a “magnetic brake”, A series of coils providing power to the rest of the ship, located in front of the detonation point (as the alpha particles first fly towards the spacecraft). Magnetic brakes directly convert the kinetic energy of charged particles into electric current at an extremely high efficiency. This is also not explored due to the challenge of cooling the coil and its exposure to high neutron flux, but can be considered as a modifiable parameter of the driver.

5. Neutron Embrittlement from >14 MeV High Energy Neutrons

Neutrons of over 14 MeV cause embrittlement and activation. Micro-abrasions in the material's crystal structure embrittle the exposed driver components [1, 15]. For continuous propulsion, constant bombardment of high energy neutrons is unacceptable for the exposed driver components, therefore a system must be in place to significantly reduce neutron flux. Reduction of neutron flux not only reduces exposure and increases engine lifetime, but also reduces the mass of shielding material, and increases the engine alpha (kg/kw) of the driver.

A possible (and here implemented) method of neutron flux reduction is through nuclear spin alignment (Spin polarization). In a D-T fusion reaction, neutrons are emitted in all directions not because the momentum transfer is random, but because the atoms are facing random directions. The neutron will always escape on the exact opposite side of the alpha particle. Atoms can be spin-polarized with a strong magnetic field, but effective spin polarization can only happen at very low energies. A freezing unit cooling the atoms in a fusion pellet to sub-microkelvin temperatures while exposing it to a ~10 Tesla magnetic field could allow nearly complete spin polarization of the fusion pellet. This polarization step would make the direction of the emitted neutron predictable, and semi-collimated into a particle beam. To balance the momentum transfer, the charged alpha particle will be emitted in the opposite direction, re-directed by a magnetic nozzle to produce thrust.

6. Implementation of a Lithium / Lithium Deuteride Tritium breeder

Additional neutron flux can be reduced with the use of a Tritium breeder, A Tritium breeder jacket can be implemented and installed in front of the Graphite-Boron-10-Aluminium radiation shield. The neutron exposure and reflected neutrons will produce Tritium and Helium:

$$Li^{6} + n \rightarrow T + {}^{4}He$$

The Tritium is to be separated and used for later reactions, while the Helium is injected into the exhaust to provide additional thrust.

The effectiveness of a Tritium breeder jacket may vary, as TaHfC and other Tantalum based alloys are excellent neutron shielding material due to its high density [16], therefore such a system can only be installed if the heat shield is thin enough to allow an acceptable level of pass-through. A breeder cannot be installed directly on, in front, or behind the heat shield to maximize the radiating area of the heat shield, allowing additional fusion power output while maintaining thermal equilibrium. If an additional hollow cylindrical breeder jacket is installed along

the end of the heat shield to absorb enough neutrons, Lithium Deuteride can be used as a single compound fuel. Upon entering the Tritium breeding jacket, Lithium-6 will absorb a neutron, splitting into Tritium and Helium. Tritium and Deuterium will be used for the following fusion reaction while the Helium is injected into the exhaust gas flow to increase thrust.

Lithium can also be directly injected into the exhaust near the heat shield to directly reduce neutron flux to the heat shield and increase thrust, creating a “fusion afterburner”. Activated Lithium may produce additional tritium that can react (which increases neutron flux as they aren’t spin-polarized), and activated Lithium will have a lowered molecular weight (Tritium and Helium), producing a theoretically greater exhaust velocity.

7. Thermal Mechanics and the Heat Shield

The major advantage of laser-inertial confinement is the open reaction chamber, therefore minimal heat transfer is made between the fusion plasma and driver components. High-energy fusion plasma is not perfectly contained by the magnetic fields, therefore the reduction of contact will not only reduce heat transfer, but also reduce micro-abrasion from charged particles and neutron embrittlement. To maximize the advantages of laser-inertial confinement, the reaction chamber will be half-open. The exact geometry is an icosahedral hollow hemisphere. The tiles of TaHfC are slightly interlocking/overlapping, and are attached to each other (and the spacecraft) with an insulated support structure behind the tiles. The heat shield assembly will also act as a central structural element, with its supports being attached to the thrust structure through the 3 Tesla plasma redirection coil.

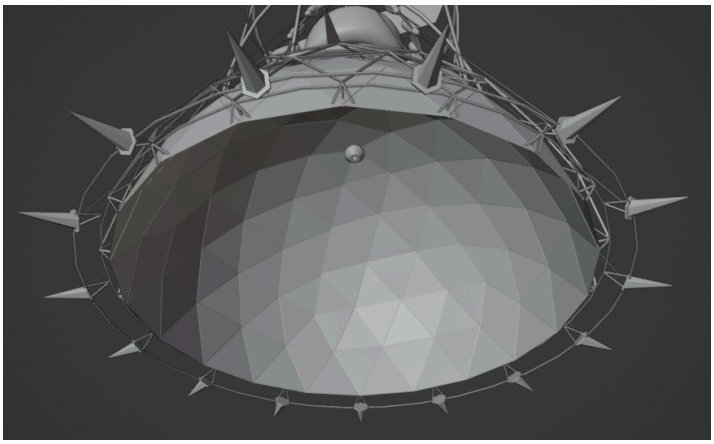

[Fig. E Icosahedral Heat Shield Geometry]

The heat shield will operate in thermal equilibrium at ~4000K. TaHfC is capable of radiating ~14.5MW/m² [1], a 10 m ⌀ (inner) heat shield with 5 mm thickness the ideal total radiated heat is ~5.7 GW [14.5 MW/m²*(78.7m²+314.79m²)]. With the detonation point at the end of the nozzle, the maximum fusion power would be ~20.74 GW [5.7GW/0.275]. A pellet injector capable of injections at 60 m/s will allow a pulse rate of 12 Hz, and a pulse unit energy of 1.7283 GJ [20.74GW/12Hz]. Fuel pellet mass of ~5.12848 milligrams. The resulting laser pulse power requirement will be 4.91 MJ [1.7283/(17,600/50)]. For fuel pellet detonation reliability, the laser pulse power will be 50% higher at 7.365 MJ.

8. Driver Theoretical Statistics Analysis

[6.1] Base Performance on Reaction Products

Exhaust Velocity (V_e)	19,343,213.8	m/s	$\sqrt{(2 * F_p')/\dot{m}}$
Thrust (F)	1190.4	N	$\dot{m} * V_e$
Mass Flow ($\dot{m}$)	6.154176e-5	kg/s	12(5.12848e-6)
Fusion Power (P_f)	20.74	GW	[14.5*(78.7+314.79)]/0.275
Thrust Power (F_p)	15.0365	GW	$P_f * 0.725$
Effective Fp with cos loss (F_p')	11.51323	GW	$0.2F_p + cos\,45°(0.8F_p)$
Specific Impulse (I_{sp})	1,972,458.87	s	$V_e/9.80665$

[6.2] Installation of Afterburner (0.025kg/s, 0.05kg/s, 0.075kg/s)

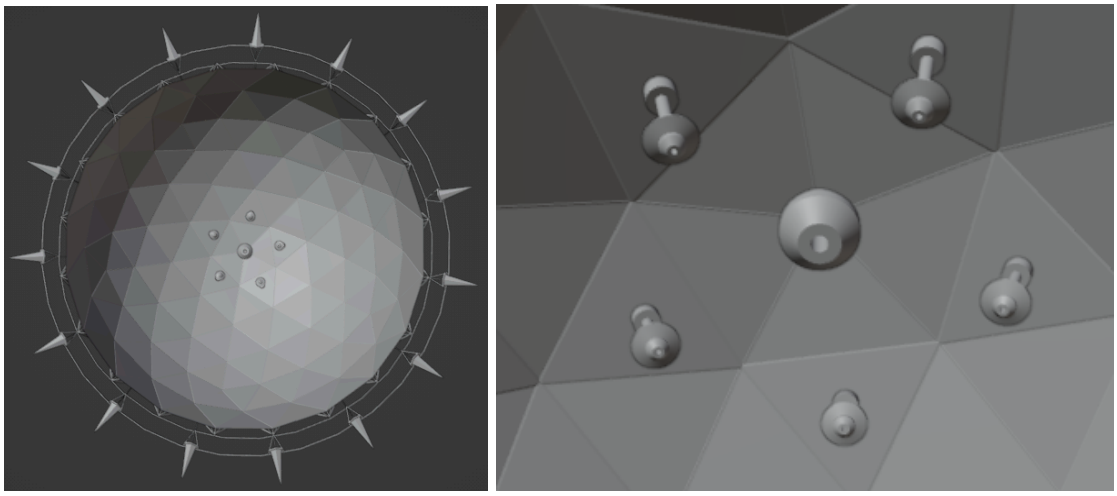

[Fig. G-1,2 Layout of Afterburner Injectors]

[Additional reaction mass injection 0.025kg/s]

Afterburning Exhaust Velocity (V_e)	958,538.8	m/s	$\sqrt{(2 * F_p')/\dot{m}'}$
Afterburner Thrust (F)	24,022	N	$\dot{m}' * V_e$
Mass Flow ($\dot{m}$)	6.154176e-5	kg/s	12(5.12848e-6)
Afterburning Mass Flow ($\dot{m}$')	0.0250615418	kg/s	$\dot{m}$ + 0.025
Effective F_p with cos loss (F_p')	11.51323	GW	$0.2F_p + cos\,45°(0.8F_p)$
Afterburner Specific Impulse (I_{sp})	97,743.76	s	$V_e/9.80665$

[Additional reaction mass injection 0.05kg/s]

Afterburning Exhaust Velocity (V_e)	678,205.77	m/s	$\sqrt{(2 * F_p')/\dot{m}'}$
Afterburner Thrust (F)	33,952	N	$\dot{m}' * V_e$
Mass Flow (ṁ)	6.154176e-5	kg/s	12(5.12848e-6)
Afterburning Mass Flow (ṁ')	0.0500615418	kg/s	ṁ + 0.05
Effective F_p with cos loss (F_p')	11.51323	GW	$0.2F_p + cos\,45°(0.8F_p)$
Afterburner Specific Impulse (I_{sp})	69,157.74	s	$V_e/9.80665$

[Additional reaction mass injection 0.075kg/s]

Afterburning Exhaust Velocity (V_e)	553,866.2	m/s	$\sqrt{(2 * F_p')/\dot{m}'}$
Afterburner Thrust (F)	41,574	N	$\dot{m}' * V_e$
Mass Flow (ṁ)	6.154176e-5	kg/s	12(5.12848e-6)
Afterburning Mass Flow (ṁ')	0.0750615418	kg/s	ṁ + 0.05
Effective F_p with cos loss (F_p')	11.51323	GW	$0.2F_p + cos\,45°(0.8F_p)$
Afterburner Specific Impulse (I_{sp})	56,478.63	s	$V_e/9.80665$

[6.3] Driver Mass Estimation

Heat Shield 5mm (TaHfC)	21.384	Tons	13.6 g/cm³ [19]
Heat Shield Structural Elements	~4	Tons	Estimation
Insulation	~800	kg	Estimation
Graphite-Boron10-Aluminium Radiation Shield	~5	Tons	Man-safe shadow shield estimation
Structural Elements	~5	Tons	Estimation
Fuel Pellet Producer	~800	kg	Estimation
Pellet Injector	~200	kg	Estimation
10 Tesla Spin-Polarization Coil (Nb-Ti)	~50	Tons	Estimated from [17]
3 Tesla Magnetic Nozzle Coil (Nb-Ti)	~8	Tons	Estimated from [17]
Cryogenic Coolant (Lqd He)	~400	kg	Estimated from [18]
Auxiliary Thermal Control	~500	kg	Estimate of Ti Radiators
Thermal Control Loops	~4+0.5	Tons	Estimate Loops + Coolant
Laser and Associated Electrical Systems	~10.1	Tons	7014 kg from 0.7kw/kg
Tritium Breeder Config 1 (not included)	~600	kg	Estimation
Tritium Breeder Config 2 (not included)	~1400	kg	Estimation
Total Driver Mass (M_{driver})	110.684	Tons	Sum of above excluding T-breeder.
Engine alpha (kg/kw)	9.614e-3	kg/kw	$M_{driver}/F_p{}'$
T/W (Reaction Products)	~1.12e-3	N/A	$F/Total\ Mass$
T/W (0.025kg/s Afterburner)	~0.0227	N/A	$F/Total\ Mass$
T/W (0.05kg/s Afterburner)	~0.0322	N/A	$F/Total\ Mass$
T/W (0.075kg/s Afterburner)	~0.0383	N/A	$F/Total\ Mass$

[6.4] Driver Power Requirement

Laser Power Requirement	~196	MW	50% Efficiency
Superconductor Cryostat	~4	MW	Estimation
Fuel Pellet Freezer & Production	~3	MW	Estimation
Thermal Loop Pumps	~7	MW	Estimation
Total Power Requirement	~210	MW	Sum of above

9. Future Mission Applications

Earth-to-Mars missions through the Hohmann Transfer take 8-9 months (one way) [22]. With NASA's NEP concepts bringing the round trip travel times to below a 2 year time frame [23]. NTP shows great promise, with a ΔV of 4200m/s [24] it could achieve travel times in ~2 years, with an engine Isp of 875s [24]. The "Pulsar" can reach Isp of >56ks with 0.075kg/s of afterburner fuel injection, making it easily surpass NEP and NTP Mars transfer vehicle options, easily bringing the one-way travel time down to >3 months (in an ideal transfer window). This brings the time frame of a manned martian mission down to >6 months.

Similar to the VISTA Fusion drive, Earth-to-Jupiter, and Earth-to-Saturn missions can also be attainable within a reasonable time frame when compared to chemical, NEP and NTP options. Manned Earth-to-Jupiter round trips can be completed within 15 months [3], while Earth-to Saturn round trips can be completed in slightly >2 years [3]. This reduction in travel time not only makes manned missions significantly more feasible, but also brings an option to deliver large probes to the outer planets in a short time frame. However, the "Pulsar" fusion driver significantly outperforms the VISTA fusion drive, with >56ks of Isp and ideal alpha of 0.0096, compared to the effective Isp of VISTA D-T of ~15ks and ideal alpha of 0.104 [3].

10. Conclusion

The “Pulsar” laser-inertial confinement fusion drive makes a promising fusion driver for the application of interplanetary travel in the near future. Significantly reducing travel times to both the inner and outer planets. Recent technological advancements in laser technology and material science significantly reduced the power requirement therefore generator / reactor mass, and thermal equilibrium, reducing mass of thermal management systems. The theoretical alpha performance of the driver “Pulsar” significantly outperformed similar concepts, while using near future or off the shelf materials and technologies.

[REFERENCES]

1. Matter Beam,. (2019, October 5). *The expanse’s Epstein Drive*. The Expanse’s Epstein Drive. https://toughsf.blogspot.com/2019/10/the-expanses-epstein-drive.html
2. Momota, H., Ishida, A., Kohzaki, Y., Miley, G. H., Ohi, S., Ohnishi, M., ... & Tuszewski, M. (1992). Conceptual design of the D-3He reactor ARTEMIS. *Fusion Technology*, *21*(4), 2-11.
3. Orth, C. D. (2005). *VISTA--A Vehicle for Interplanetary Space Transport Application Powered by Inertial Confinement Fusion* (No. UCRL-TR-110500). Lawrence Livermore National Lab.(LLNL), Livermore, CA (United States).
4. Brady, P. (2025, July 13). *Laser glass*. National Ignition Facility & Photon Science. https://lasers.llnl.gov/about/seven-wonders/laser-glass
5. Meaney, K. D., Kim, Y., Geppert-Kleinrath, H., Herrmann, H. W., Moore, A. S., Hartouni, E. P., ... & Church, J. A. (2021). Total fusion yield measurements using deuterium–tritium gamma rays. *Physics of Plasmas*, *28*(10).
6. Rider, T. H. (1994). *A general critique of inertial-electrostatic confinement fusion systems* (Doctoral dissertation, Massachusetts Institute of Technology), 38-40.
7. Evans, J. (2023, July 26). *Traveling to the sun: Why won’t Parker Solar Probe Melt?* NASA. https://www.nasa.gov/solar-system/traveling-to-the-sun-why-wont-parker-solar-probe-melt/
8. Bruhaug, G., & Kish, A. (2024). Benefits of Spin Polarization for Inertial and Magneto-Inertial Fusion Propulsion. *Journal of Propulsion and Power*, *40*(1), 164-168.
9. Robert S. (2019, June 20). Fusion Propulsion Technology for Interstellar Missions, Interstellar Exploration Workshop -ESTEC

10. Shumlak, U., Lilly, R., Adams, C., Golingo, R., Jackson, S., Knecht, S., & Nelson, B. A. A. E. R. P. (2006). Advanced space propulsion based on the flow-stabilized Z-pinch fusion concept. In *42nd AIAA/ASME/SAE/ASEE Joint Propulsion Conference & Exhibit* (p. 4805).
11. Zhang, Y., Shumlak, U., Nelson, B. A., Golingo, R. P., Weber, T. R., Stepanov, A. D., ... & Cooper, C. M. (2019). Sustained neutron production from a sheared-flow stabilized Z pinch. *Physical review letters*, *122*(13), 135001.
12. Cramer, J. G. (2016, June 30). The Direct Fusion Drive Rocket. https://www.npl.washington.edu/av/altvw185.html
13. Patwardhan, K. V., Patwardhan, A. W., Gaikar, V. G., & Bhaskaran, M. (2007). Modeling of monothermal ammonia–hydrogen chemical exchange column using a non-equilibrium model. *Chemical engineering science*, *62*(15), 4077-4094.
14. Forward, R. (1985). Antiproton annihilation propulsion. *Journal of Propulsion and Power*, *1*(5), 370-374.
15. Stainer, T., Gilbert, M. R., Packer, L. W., Lilley, S., Gopakumar, V., & Wilson, C. (2021). 14 MeV neutron irradiation experiments-gamma spectroscopy analysis and validation automation. In *EPJ Web of Conferences* (Vol. 247, p. 09010). EDP Sciences.
16. Giménez, M. A. N., & Lopasso, E. M. (2018). Tungsten carbide compact primary shielding for small medium reactor. *Annals of Nuclear Energy*, *116*, 210-223.
17. SAAN. (2020, June 26). *Installation of 9.4 tesla MRI on Maastricht Health Campus*. https://www.saan.nl/en/projecten/installation-of-9-4-tesla-mri-on-maastricht-health-campus/
18. Roshini, T. V., & Subramaniam, K. (2016). Laser cooling system for magnetic resonance imaging scanner using normal controller. *Int J Comput Appl*, *975*, 36-40.
19. Rudy, E., & Nowotny, H. (1963). Untersuchungen im system hafnium-tantal-kohlenstoff. *Monatshefte für Chemie und verwandte Teile anderer Wissenschaften*, *94*, 507-517.
20. Ishida, A. (2020). Formula for energy conversion efficiency of thermoelectric generator taking temperature dependent thermoelectric parameters into account. *Journal of Applied Physics*, *128*(13).
21. EAGLE Lasers. (2025, August 16). *Fiber vs. CO2 Laser*. https://eagle-group.eu/en/fiber-vs-co2-laser
22. Kayton, M. (2026, August 6). *Hohmann Transfer Orbit Diagram*. Hohmann transfer orbit diagram. https://www.planetary.org/space-images/hohmann-transfer-orbit
23. NASA. (2025, January 31). *From Earth to Mars in two years? NASA's nuclear solution*. SciTechDaily. https://scitechdaily.com/from-earth-to-mars-in-two-years-nasas-nuclear-solution/
24. Nikitaeva, D., & Thomas, L. (2021). In-Situ Alternative Propellants for Nuclear Thermal Propulsion. In *AIAA Propulsion and Energy 2021 Forum* (p. 3597).